J. Nanoanalysis., 5(2): 130-137 Spring 2018

ORIGINAL RESEARCH PAPER

Preparation of $CdIn_2S_4$-CdS nanocomposite via a green route and using them in dot-sensitized solar cells for boosting efficiency

Mehdi Mousavi-Kamazani

New Technology Faculty, Semnan University, Semnan, Iran

Received: 2018-05-20 Accepted: 2018-06-10 Published: 2018-06-30

ABSTRACT

In this work In_2S_3 and CdS nanoparticles were prepared by a simple hydrothermal method and then annealed at 500 °C for 2 h in an Ar gas until $CdIn_2S_4$(CdIS)-CdS nanocomposites were formed. Afterward, the efficiency of the as-synthesized CdIS-CdS nanocomposite in quantum dot-sensitized solar cells (QDSSCs) was evaluated. For this purpose, the as-prepared CdIS-CdS nanocomposites were deposited on TiO_2 by doctor's blade technique and electrophoresis deposition was used for fabrication of TiO_2 layer on the FTO glass substrate. Using CdIS-CdS nanocomposite led to obtaining 1.71% cell efficiency that in comparison with pure CdS (0.97%) and $CdIn_2S_4$ nanoparticles (95%), efficiency improvements of 76% and 80% were respectively achieved.

Keywords: *$CdIn_2S_4$-CdS, Nanocomposite, QDSSCs, Thermal Decomposition*

How to cite this article

Mousavi-Kamazani M. Preparation of $CdIn_2S_4$-CdS nanocomposite via a green route and using them in dot-sensitized solar cells for boosting efficiency. J. Nanoanalysis., 2018; 5(2): 130-137. DOI: 10.22034/jna.2018.541870

INTRODUCTION

Semiconductor quantum dots (QDs) have attracted significant attention as possible candidates to increase the energy conversion efficiency of solar cells. Typically, the utilization of a multiple exciton generations (MEG) of QDs is expected to increase the power (PCE) of a single-junction solar cell beyond the Shockley-Queisser limit to 44% [1-4]. Among the third-generation solar cells based on quantum dots, quantum dot sensitized solar cells (QDSSC) have been studied using a variety of semiconductors including CdSe, CdTe, CdS, PbS, PbSe, Bi_2S_3, InP and so on [5-12]. QDSSCs possess some attractive advantages include: high absorption cross section, bandgap tunability from the infrared to the ultraviolet region through control of their composition and size, high extinction coefficients, the potential of high power conversion efficiency (PCE) based on the generation of multiple excitons by the impact-ionization effect in QDs [13-16] and the relative simplicity of their synthesis from low cost solution methods [17-19]. Thus, QDSSCs have been considered as a promising candidate of the third generation solar cells, and so the related research papers remarkably increased. However, there are a few reports on the composites of these materials such as $CuInS_2$-Cu_2S, $AgInS_2$-Ag_2S, and $CdIn_2S_4$-CdS and this can have various reasons such as reporting no suitable method to synthesize their composites (in most of approaches for synthesizing such as solvothermal-hydrothermal, pure phase of them will be formed), lack of knowledge about their amazing properties and pay too much attention to pure materials. In our previous study, we synthesized $CuInS_2$-Cu_2S nanocomposite via a green simple hydrothermal method and the results showed that nanocomposites have better efficiency in solar cells compared to pure substances [20]. Connor and et al. [21] synthesized the preparation of Cu_2S-CIS heterostructured NRs by colloidal solution-phase growth. They showed that the biphasic NRs can be easily converted to monophasic

* Corresponding Author Email: *m.mousavi@semnan.ac.ir*

NRs at temperatures above 250 °C due to their similar crystal structures and fast diffusion of Cu(I) ions in the superionic state. Their results revealed that Cu_2S-CIS shows better optical properties than each of Cu_2S or CIS alone and this can be useful in optical applications.

In this present work, we conducted the CdIS-CdS nanocomposite preparation using simple, low-cost and solvent-less route via thermal decomposing the mixture of In_2S_3 and CdS under argon atmosphere at 500 °C. For this purpose, In_2S_3 and CdS were produced by hydrothermal method. Then, the as-prepared CdIS-CdS nanocomposite were deposited on TiO_2 by doctor's blade technique and the short-circuit photocurrent density (J_{sc}), open-circuit voltage (V_{oc}), fill factor (FF) and efficiency of solar cell was studied. Moreover, the synthesized $CdIn_2S_4$-CdS nanocomposites were applied as a barrier layer in DSSCs.

EXPERIMENTAL

Materials and physical measurements

Commercially-available TiO_2 powder of P25 (av. 30 nm by Brunauer-Emmett-Teller (BET), 80% anatase (d=21 nm) and 20% rutile (d=50 nm), via $TiCl_4$-fumed gas synthesis, Degussa, Germany), 4-tert-butylpyridine (4-tBP) (Aldrich), acetonitrile (Fluka), valeronitrile (Fluka), H_2PtCl_6 (Fluka), Iodine (I2) (99.99%, Superpur1, Merck), lithium iodide (LiI) (Merck), acetyl acetone (acac) (Merck), $Cd(NO_3)_2$ (Aldrich), $InCl_3$ (Aldrich), thioacetamide (Aldrich), FTO glass (TEC-15, Dyesol) and ethanol (Merck) were used as received. H_2O was purified by distillation and filtration (Milli-Q). X-ray diffraction (XRD) patterns were recorded by a Philips-X'PertPro, X-ray diffractometer using Ni-filtered Cu Kα radiation at scan range of $10<2\theta<80$. The energy dispersive spectrometry (EDS) analysis was studied by X-Max oxford, Philips microscope. Scanning electron microscopy (SEM) images were obtained on LEO-1455VP equipped with an energy dispersive X-ray spectroscopy. The diffused reflectance UV-visible spectra (DRS) of the samples was recorded by an Ava Spec-2048TEC spectrometer. Photocurrent density-voltage (J-V) curve was measured by using computerized digital multimeters (Ivium-n-Stat Multichannel potentiostat) and a variable load. A 300 W metal xenon lamp (Luzchem) served as assimilated sun light source, and its light intensity (or radiant power) was adjusted to simulated AM 1.5 radiation at 100 mW/cm^2 with a filter for this purpose.

Synthesis of In_2S_3, CdS, and $CdIn_2S_4$ nanoparticles via hydrothermal route

In_2S_3: In a typical experimental procedure, 2 mmol of $InCl_3$, 3 mmol of thioacetamide (TAA), and 0.05 g of cetyltrimethylammonium bromide (CTAB) were mixed in 30 ml of distilled water and stirred for 10 min. The final solution was transferred to the 150 ml Teflon-lined stainless steel autoclave maintained at 160 °C for 10 h and then the autoclave was allowed to cool down to room temperature naturally. The obtained product was centrifuged and washed with absolute ethanol and distilled water several times and was dried at 70 °C for 10 h [20].

CdS: 1 mmol of $Cd(NO_3)_2.4H_2O$ and 0.05 g of CTAB were suspended to 40 ml of distilled water under stirring. After 10 min, 1 mmol of TAA was added and the final solution was transferred to the 150 ml Teflon-lined stainless steel autoclave maintained at 180 °C for 10 h [22].

$CdIn_2S_4$: 1 mmol of $Cd(NO_3)_2.4H_2O$, 2 mmol of $InCl_3$, 4 mmol of thioacetamide (TAA), 2 ml of NaOH, and 0.05 g of CTAB were mixed in 30 ml of distilled water and stirred for 10 min. The final solution was transferred to the 150 ml Teflon-lined stainless steel autoclave maintained at 180 °C for 10 h. The obtained precipitate was washed with deionized water and ethanol, and was dried at 70 °C for 10 h.

Synthesis of $CdIn_2S_4$-CdS nanocomposite

The starting powders including 0.5 g of In_2S_3 and 0.5 g of CdS were milled and mixed in a ball mill for 10 min using zirconia grinding media. Afterwards, the powder mixtures were calcined at 500 °C for 2 h under argon atmosphere. Finally, it was washed with distilled water and absolute ethanol several times and dried at 70 °C for 10 h (sample 1). For investigation of temperature effect on morphology and purity of final product an experiment was performed at 600 °C for 2 h under argon atmosphere (sample 2). Also, an experiment was performed with the same above procedure (at 500 °C for 2 h) under atmospheric condition (sample 3).

Fabrication of FTO/TiO_2/$CdIn_2S_4$-CdS/Pt-FTO Cell

Electrophoresis deposition (EPD) was utilized to the prepare TiO_2 films [23]. During EPD, the cleaned FTO glass remained at a positive potential (anode) while a pure steel mesh was used as the counter (cathode) electrode. The linear distance

between the two electrodes was about 3 cm. Power was supplied by a Megatek Pro-grammable DC Power Supply (MP-3005D). The applied voltage was 10 V. The deposition cycle was repeated 4 times, each time 5s, and the temperature of the electrolyte solution was kept constant at 25 °C. The coated substrates were air dried. The apparent area of the film was 1 × 1 cm^2. The resulted layer was annealed under an air flow at 500 °C for 30 min. Electrolyte solution consisted of 120 mg/l of I_2, 48 ml/l of acetone, and 20 ml/l of water. For deposition of $CdIn_2S_4$-CdS powder on the FTO glass substrate, a paste of CdIS-CdS was initially prepared. The slurry was produced by mixing and grinding 1.0 g of the nanometer sized $CdIn_2S_4$-CdS with ethanol and water in several steps. Afterwards, the ground slurry was sonicated with ultrasonic horn (Sonicator 3000; Bandeline, MS 72, Germany) and then mixed with terpineol and ethyl cellulose as binders. After removing the ethanol and water with a rotary-evaporator, the final paste was prepared. The prepared CdIS-CdS paste was coated on TiO_2 film by a doctor blade technique. After that the electrode was gradually heated under an air flow at 450 °C for 30 min. Counter-electrode was made from deposition of a Pt solution on FTO glass. Afterward, this electrode was placed over TiO_2/CdIS-CdS electrode. Sealing was accomplished by pressing the two electrodes together on a double hot-plate at a temperature of about 110 °C. The I_3/I^- electrolyte was introduced into the cell through one of two small holes drilled in the counter electrode. Finally, these two holes were sealed by a small square of sealing sheet and characterized by J-V test.

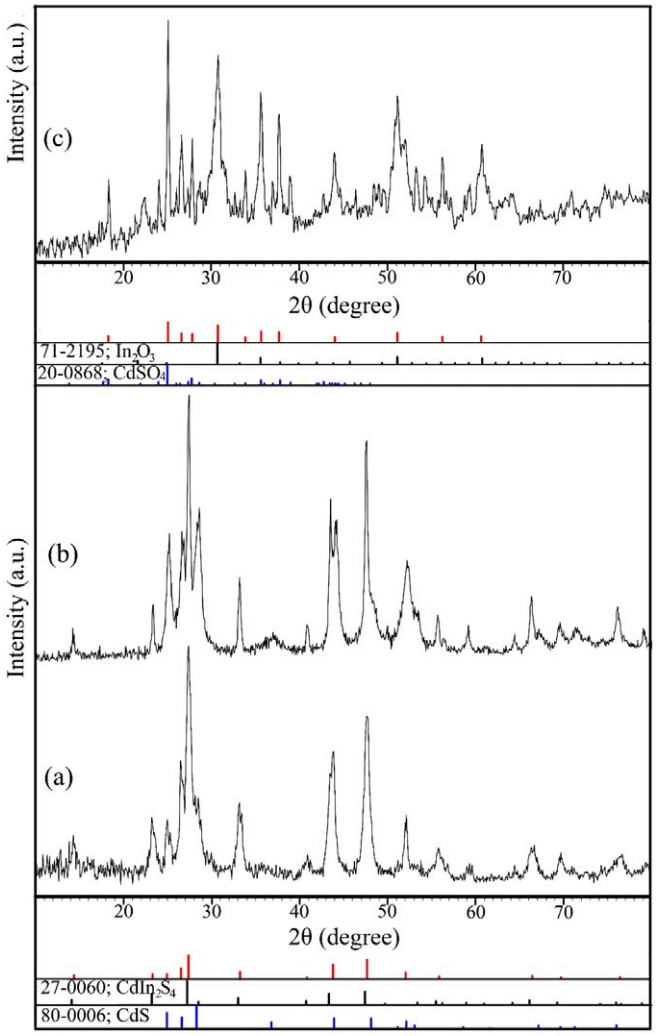

Fig. 1. XRD pattern of the as-obtained products (a) at 500 °C under argon atmosphere (sample 1), (b) at 600 °C under argon atmosphere (sample 2), and (c) at 500 °C under atmospheric condition (sample 3).

RESULTS AND DISCUSSION

The crystal structure and phase composition of the products were characterized by powder X-ray diffraction pattern. XRD pattern of the as-obtained products via solid-state thermal decomposition of the mixed In_2S_3 and CdS powders at 500 °C for 2 h under argon atmosphere (sample 1), at 600 °C for 2 h under argon atmosphere (sample 2), and at 500 °C for 2 h under atmospheric condition (sample 3) are presented in Figs. 1a-c, respectively. As can be seen, in presence of argon gas at 500 °C (Fig. 1a), mixture of CdS and $CdIn_2S_4$ was prepared and there is no amount of In_2O_3 and CdO as impurities. The similar results were found by conducting the experiment at 600 °C (sample 2) but decreasing of width of peaks shows growth of particles (Fig. 1b). As shown in Figs 1a and b, two sets of diffraction peaks which can be indexed to cubic phase of $CdIn_2S_4$ (JCPDS No. 27-0060, space group: Fd3m and calculated cell parameter a = 10.8450 Å) and hexagona phase of CdS (JCPDS No. 80-0006, space group: P63mc and calculated cell parameter a = b = 4.1210 Å and c = 6.6820) are observable. When a stoichiometric amount of CdS and In_2S_3 is used, we expect as below mechanism that pure phase of $CdIn_2S_4$ can be prepared [24, 25]. In this paper, the ratio 1 to 1 was not used because the purpose was composite production.

$$CdS + In_2S_3 \rightarrow CdIn_2S_4$$

By performing the experiment in absence of argon gas (sample 3), mixture of impurities including In_2O_3 and $CdSO_4$ instead of desired product ($CdIn_2S4$-CdS) was prepared (Fig. 1c). These results show for obtaining the desired product by annealing In_2S_3 and CdS, presence of argon gas is necessary.

From XRD data, the crystallite diameter (Dc) of sample 1 was calculated to be 14 nm using the Scherrer equation [26, 27]:

$$D_c = K\lambda/\beta\cos\theta \qquad \text{Scherrer equation}$$

Where D is the crystallite size, as calculated for the (hkl) reflection, λ is the wavelength of Cu Kα radiation (0.154 nm), θ is the Bragg diffraction angle, k is a constant related to the crystal shape (0.94), and β is the full width at half maximum (FWHM) of the peak appearing at the diffraction angle of theta. Energy dispersive X-Ray analysis (EDX) was used to identify the elemental composition and chemical purity of obtained products. Fig. 2 shows typical EDX spectrum of the as-prepared $CdIn_2S_4$-CdS nanocomposite (sample 1). As can be seen in Fig. 2, only Cd, In ,and S peaks exist in the mentioned nanocomposite except for the peak due to the use of Au-coated substrate for samples examination which indicate the obtained nanocomposite is without any impurity such as CdO, In_2O_3 and $CdSO_4$. The morphology of the as-synthesized samples was revealed by scanning electron microscopy (SEM). Figs. 3a-d, show the SEM images of samples 1 and 2 which prepared from annealing of CdS and In_2S_3 under argon gas at 500 °C and 600 °C, respectively. As shown, in both of conditions the nanoparticles were obtained but the sample 2 (annealed at 600 °C) has larger nanoparticles compared with sample 1 (annealed at 500 °C). The UV-Vis absorption spectra of bare TiO_2, TiO_2/CdS, TiO_2/CdIS, and TiO_2/CdIS-CdS (sample 1) are shown in Fig. 4. As can be seen, intensity of absorption edge for TiO_2/CdIS-CdS is more than other samples. These results show

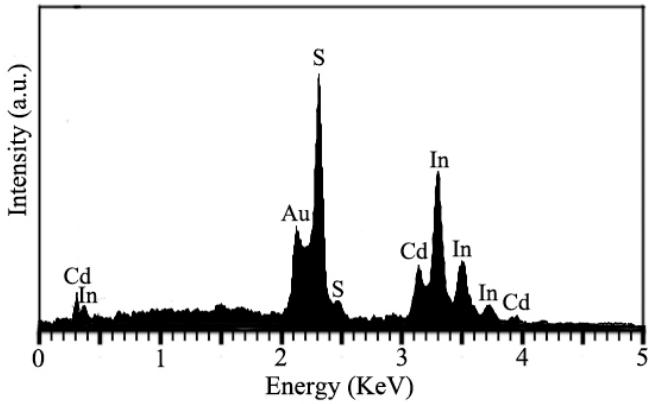

Fig. 2. EDS spectrum of the as-prepared CdIS-CdS nanocomposite (sample 1).

that by depositing the CdIS-CdS on TiO_2 surface, light harvesting in the visible light region can be improved and so the efficiency of solar cell will be enhanced. For comparing the efficiency of QDSSCs fabricated from different samples, current density-voltage (J-V) curves were obtained and their short-circuit current density (J_{SC}), open-circuit voltage (V_{OC}), fill factor (FF) and the corresponding overall power conversion efficiency (η) parameters are presented in Fig. 5 and Table 1. As can be seen, the maximum value of efficiency (1.71%) is related to CdIS-CdS nanocomposite and lowest efficiency (0.24%) was achieved for In_2S_3 nanoparticles. J_{SC} and V_{OC} parameters were well improved using CdIS-CdS nanocomposite compared to pure In_2S_3, $CdIn_2S_4$, and CdS and eventually more efficiency

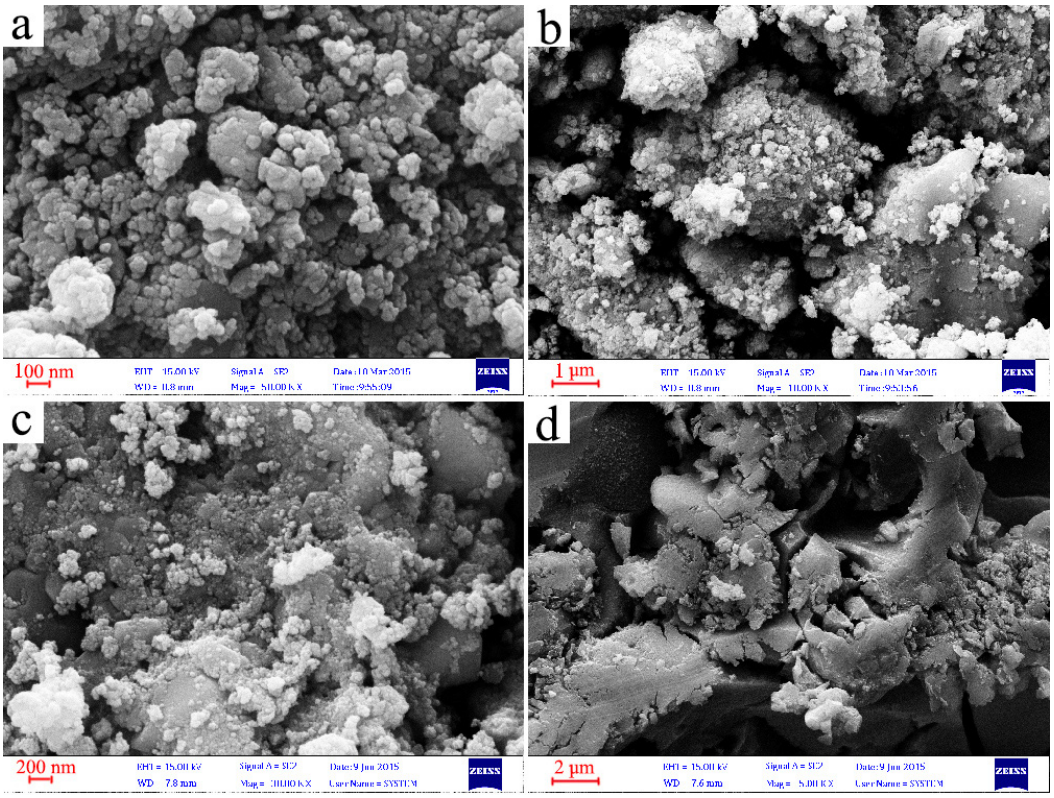

Fig. 3. Different scales of SEM images of the as-synthesized (a) and (b) sample 1, (c) and (d) sample 2.

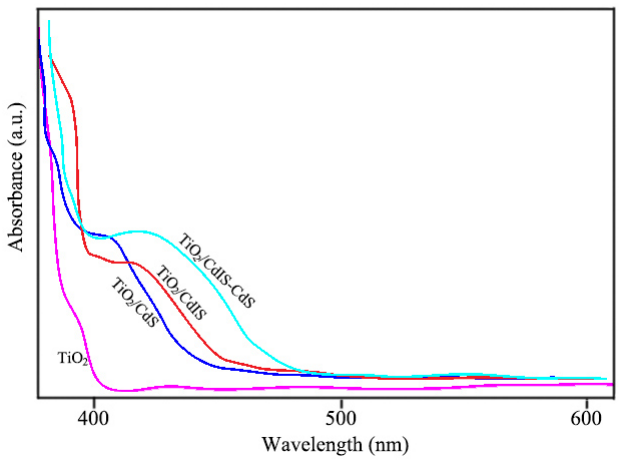

Fig. 4. UV-Vis diffuse reflectance spectroscopy of bare TiO_2, TiO_2/CdS, TiO_2/CdIS, and TiO_2/CdIS-CdS.

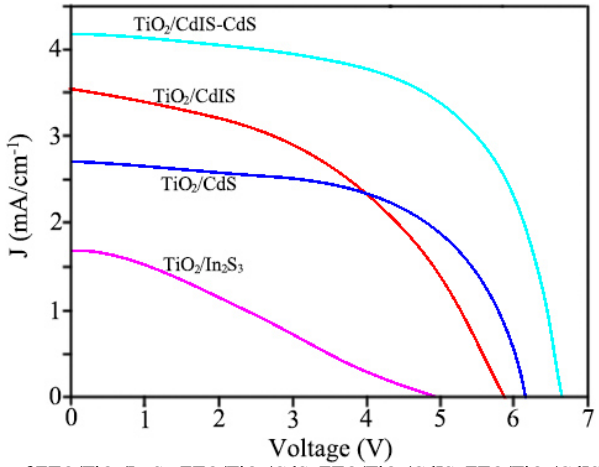

Fig. 5. J-V curves of FTO/TiO_2/In_2S_3, FTO/TiO_2/CdS, FTO/TiO_2/CdIS, FTO/TiO_2/CdIS-CdS electrodes.

Table 1. J-V characterization results of the as-prepared QDSSCs.

Cell No.	V_{oc} (V)	J_{sc} (mA/cm^2)	FF	η (%)
TiO_2/In_2S_3	0.52±0.02	1.71±0. 1	0.27±0.6	0.24
TiO_2/CdS	0.61±0.02	2.71±0.2	0.59±0.4	0.97
TiO_2/CdIS	0.58±0.02	3.56±0.2	0.46±0.4	0.95
TiO_2/CdIS-CdS	0.66±0.03	4.11±0.3	0.63±0.3	1.71

will be obtained. According to solar cells efficiency equation (1) indicated as follow:

$$\eta = J_{sc} \times V_{oc} \times {}^{FF}/_{I_0} \times 100 \qquad (1)$$

The higher V_{OC} and J_{SC} values result in higher efficiency. V_{OC} value is related to difference between Fermi levels of p and n junction bands. CdIS-CdS nanocomposite compared to pure CdS or $CdIn_2S_4$ has higher difference between Fermi levels. J_{SC} value is related to absorption and with increasing of absorption value, the J_{SC} will increase. About 47% of solar radiations exist in IR area, 46% within the visible range and 7% in UV band. Therefore, the bandgap of materials should be such that absorbs in the IR and visible areas. According to Fig. 4, CdIS-CdS nanocomposite has higher absorption and therefore higher J_{SC} is expected for it. The achieved value of efficiency for CdIS-CdS nanocomposite showed 76% improvement compared to CdS and 80% improvement compared to $CdIn_2S_4$ that can be related to more efficient light harvesting of $CdIn_2S_4$-CdS nanocomposite.

CONCLUSION

In the present work, for the first time, CdIS-CdS nanocomposite has been synthesized via a green solid-state thermal decomposition of the mixed In_2S_3 and CdS powders at 500 °C for 2 h in an Ar gas. The obtained XRD results show that for synthesizing CdIS-CdS nanocomposite without oxide impurities, the presence of argon gas is required. SEM images also showed that the composite contains spherical nanoparticles. Then, the performance of obtained CdIS-CdS nanocomposite in quantum dot-sensitized solar cells was evaluated. The results showed CdIS-CdS nanocomposite (1.71%) has higher efficiency compared to pure In_2S_3 (0.24%), CdS (0.97%), and $CdIn_2S_4$ (0.95%) nanoparticles.

ACKNOWLEDGEMENTS

Author is grateful to the council of Iran National Science Foundation (INSF) and University of Semnan for supporting this work.

CONFLICT OF INTEREST

The authors declare that there is no conflict of interests regarding the publication of this manuscript.

REFERENCES

[1] F. Huang, J. Houc, H. Wang, H. Tang, Z. Liu, L. Zhang, Q. Zhang, S. Peng, J. Liu, G. Cao, Nano Energy, 32, 433 (2017).
[2] P. Sehgal and A.K. Narula, Electrochim. Acta, 158, 49 (2015).

[3] M.P.A. Muthalif, Y.S. Lee, C.D. Sunesh, H.J. Kim, Y. Choe, Appl. Surf. Sci., 396, 582 (2017).
[4] O.E. Semonin, J.M. Luther, S. Choi, H.Y. Chen, J. Gao, A.J. Nozik and M.C. Beard, Science, 344, 1530 (2011).
[5] H.J. Lee, J. Bang, J. Park, S. Kim and S.M. Park, Chem. Mater., 22, 5636 (2010).
[6] R.J. Ellingson, M.C. Beard, J.C. Johnson, P. Yu, O.I. Micic, A.J. Nozik, A. Shabaev and A.L. Efros, Nano lett., 5, 865 (2005).
[7] N. Parsi Benehkohal, V. González-Pedro, P.P. Boix, S. Chavhan, R. Tena-Zaera, G.P. Demopoulos and I. Mora-Seró, J. Phys. Chem. C, 116, 16391 (2012).
[8] P. Lv, W. Fu, H. Yang, H. Sun, Y. Chen, J. Ma, X. Zhou, L. Tian, W. Zhang and M. Li, Cryst. Eng. Comm., 15, 7548 (2013).
[9] J. Tian, R. Gao, Q. Zhang, S. Zhang, Y. Li, J. Lan, X. Qu and G. Cao, J. Phys. Chem. C, 116, 18655 (2012).
[10] J. Wang, I. Mora-Seró, Z. Pan, K. Zhao, H. Zhang, Y. Feng, G. Yang, X. Zhong and J. Bisquert, J. Am. Chem. Soc., 135, 15913 (2013).
[11] S.H. Im, H.-j. Kim, S.W. Kim, S.-W. Kim and S.I. Seok, Nanoscale, 4, 1581 (2012).
[12] D. Esparza, I. Zarazúa, T. López-Luke, R. Carriles, A. Torres-Castro and E. De la Rosa, Electrochim. Acta, 180, 486 (2015).
[13] V. Gonzalez-Pedro, X. Xu, I. Mora-Sero and J. Bisquert, ACS Nano, 4, 5783 (2010).
[14] P. V. Kamat, J. Phys. Chem. C, 112, 18737 (2008).
[15] W. Ma, S.L. Swisher, T. Ewers, J. Engel, V.E. Ferry, H.A. At water and A.P. Alivisatos, ACS Nano, 5, 8140 (2011).
[16] D. Segets, J. M. Lucas, R.N.K. Taylor, M. Scheele, H. Zheng, A.P. Alivisatos and W. Peukert, ACS Nano, 6, 9021 (2012).
[17] V. González-Pedro, X. Xu, I. Mora-Seró and J. Bisquert, ACS Nano, 4, 5783 (2010).
[18] S. Giménez, I. Mora-Seró, L. Macor, N. Guijarro, T. Lana-Villarreal, R. Gómez, L.J. Diguna, Q. Shen, T. Toyoda and J. Bisquert, Nanotechnol., 20, 295204 (2009).
[19] J. Jasieniak, M. Califano and S.E. Watkins, ACS Nano, 5, 5888 (2011).
[20] M. Mousavi-Kamazani, Z. Salehi and K. Motevalli, Appl. Phys. A, 123, 691 (2017).
[21] S.T. Connor, C.M. Hsu, B.D. Weil, S.Aloni and Y. Cui, J. Am. Chem. Soc., 131, 4962 (2009).
[22] M. Mousavi-Kamazani, M. Salavati-Niasari, M. Goudarzi and Z. Zarghami, J. Molecular Liquids, 242, 653 (2017).
[23] M. Mousavi-Kamazani, Z. Zarghami and M. Salavati-Niasari, J. Phys. Chem. C, 120, 2096 (2016).
[24] M. Mousavi-Kamazani, M. Salavati-Niasari, H. Emadi, Mater. Res. Bull. 47, 3983 (2012).
[25] M.T. Taghizadeh, M. Vatanparast, J. Colloid Interface Sci., 483, 1 (2016).
[26] M. Vatanparast, M.T. Taghizadeh, J. Mater. Sci.: Mater. Electron. 27, 54 (2016).